

Fuzzy Torus in Matrix Model

Subrata BAL^{a*}, Masanori HANADA^{b†}, Hikaru KAWAI^{ab‡}, Fukuichiro KUBO^{b§}^a *Theoretical Physics Laboratory, RIKEN (The Institute of Physical and Chemical Research),
Wako, Saitama 351-0198, Japan*^b *Department of Physics, Kyoto University, Kyoto 606-8502, Japan***Abstract**

We have calculated the free energy up to two loop to compare T^2 with T^4 in IIB matrix model. It turns out that T^2 has smaller free energy than T^4 . We have also discussed the generation of the gauge group by considering k -coincident fuzzy tori and found that in this case $U(1)$ gauge group is favored. This means that if the true vacuum is four-dimensional, it is not a simple fuzzy space considered here.

*E-mail address : subrata@riken.jp

†E-mail address : hana@gauge.scphys.kyoto-u.ac.jp

‡E-mail address : hkawai@gauge.scphys.kyoto-u.ac.jp

§E-mail address : kubo@gauge.scphys.kyoto-u.ac.jp

1 Introduction

IIB matrix model [1] is a candidate of the constructive definition of superstring theory. It is defined by the action

$$S = -\frac{1}{g^2} \text{Tr} \left(\frac{1}{4} [A_\mu, A_\nu] [A_\mu, A_\nu] + \frac{1}{2} \bar{\Psi} \Gamma^\mu [A_\mu, \Psi] \right), \quad (1.1)$$

where A_μ and Ψ are $N \times N$ Hermitian matrices. A_μ is a ten-dimensional vector and Ψ is a ten-dimensional Majorana-Weyl fermion.

One of the important aspects of this model is the dynamical generation of the spacetime and the gauge group. In this model the eigenvalue distribution represents spacetime geometry. From this point of view, if a four-dimensional eigenvalue distribution has smaller free energy than the other configurations, the spacetime will be compactified to four-dimensions. On the other hand the stability of k coincident D-branes may indicate the dynamical generation of $U(k)$ gauge group. So far, various attempts on this have been made. Several such attempts using branched polymer [2], complex phase effect [3] and especially improved mean-field approximation [4] were successful. In these studies, four-dimensional configurations were found to have smaller free energy.

Another interesting approach is to compare the free energies on noncommutative backgrounds. In string theory, noncommutative gauge theories on flat or curved backgrounds are realized with constant or nonconstant $B_{\mu\nu}$ [5]. IIB matrix model on flat fuzzy space backgrounds can be mapped to noncommutative super Yang-Mills theory (NCSYM) [6], and the system can be analyzed by perturbative calculations. Noncommutative gauge theories on curved manifolds have recently been studied extensively by deforming IIB matrix model [7, 8].

However, flat fuzzy space backgrounds cannot be realized as classical solutions at finite N . Therefore, in order to see the N -dependences of the free energies, we must study compact noncommutative spaces. Fuzzy S^2 , $S^2 \times S^2$ and $S^2 \times S^2 \times S^2$ backgrounds have already been studied and $S^2 \times S^2$ has been shown to be stable under certain deformations [9, 10].

In this paper, we study the free energies of IIB matrix model on fuzzy torus backgrounds. The relation to flat fuzzy space is more transparent in the case of the fuzzy torus than in the case of fuzzy sphere. We expand the action of IIB matrix model around a fuzzy torus background and sum up all 1PI diagrams. Then, we search the minimum of the free energy. Especially, we compare T^2 and T^4 backgrounds. In principle, in order to find the true vacuum, we must calculate free energies on all possible backgrounds and find the minimum. Here, however, we consider only fuzzy torus. Although fuzzy torus is not a classical solution, however, as we will show later, fuzzy torus locally looks like flat fuzzy space, which is a classical solution. Therefore, we expect our calculation captures some qualitative feature of flat fuzzy spaces. If the true vacuum is similar to a flat fuzzy space, we may find some informations such as dimensionality of the spacetime on it. In present study we will see that T^2 has smaller free energy than T^4 . This implies that if the true vacuum is four-dimensional, it is not a simple noncommutative space considered here.

Although both fuzzy sphere and fuzzy torus break supersymmetry, the breaking effect is soft and the loop corrections to their free energies almost vanish. This is because their local structures are similar to flat fuzzy spaces. In the case of fuzzy S^2 , $S^2 \times S^2$ and $S^2 \times S^2 \times S^2$, such cancellations have been confirmed to 2-loop level [9, 10]. For fuzzy torus we can see such cancellation at any loop level. Furthermore, in this case the calculations become simpler and we can study larger parameter region. For example, on T^4 , we vary the ratio r of the noncommutativity parameters of two tori and their ratio R of the matrix size ¹. We can also see the effect of the global topologies on the free energies by comparing the results for fuzzy tori and fuzzy spheres.

On the other hand, fuzzy torus has a few drawbacks. We embed fuzzy T^2 into \mathbf{R}^4 , while fuzzy S^2 can be embedded into \mathbf{R}^3 . Therefore, in ten dimensions we can realize only two- and four-dimensional configurations using fuzzy tori (T^2 and T^4), while a six-dimensional configuration can be constructed using fuzzy spheres ($S^2 \times S^2 \times S^2$). In [10] it is shown that $S^2 \times S^2$ has a smaller free energy than $S^2 \times S^2 \times S^2$. In our case, such comparison is impossible. We also have subtlety in the perturbative

¹In the case of $S^2 \times S^2$, $r^2 = R$ was studied [9].

calculation, due to the presence of a few tachyons on fuzzy torus. We will discuss this problem in detail later.

The organization of the paper is as follows. In section 2, we will construct the fuzzy torus backgrounds and show the correspondence between fuzzy torus and flat fuzzy space. In section 3, we calculate the free energy up to two loop level analytically, and in section 4, we compare the free energies numerically. In appendices, we show the detail of the calculations. Although we are interested in T^4 , we will mostly show the Feynman diagrams and calculations of T^2 as T^4 calculations are very lengthy.

2 IIB matrix model on fuzzy torus backgrounds

In order to perform a perturbative calculation, we decompose A_μ and Ψ into a background P_μ and the fluctuation a_μ, φ around it:

$$A_\mu = P_\mu + a_\mu \quad , \quad \Psi = 0 + \varphi. \quad (2.1)$$

Adding a gauge fixing and the corresponding ghost term

$$S_{\text{GF+FP}} = -\frac{1}{g^2} \text{Tr} \left(\frac{1}{2} [P_\mu, a^\mu]^2 + [P_\mu, b][A^\mu, c] \right) \quad (2.2)$$

to (1.1), we obtain the full action

$$\begin{aligned} S + S_{\text{GF+FP}} &= \frac{1}{4g^2} \text{Tr} F^2 \\ &+ \frac{i}{g^2} \text{Tr} (\mathcal{P}_\mu a_\nu) F_{\mu\nu} \\ &+ \frac{1}{g^2} \text{Tr} \left\{ \frac{1}{2} a_\mu (\mathcal{P}^2 \delta_{\mu\nu} - 2i\mathcal{F}_{\mu\nu}) a_\nu - \frac{1}{2} \bar{\varphi} \mathcal{P} \varphi + b \mathcal{P}^2 c \right\} \\ &- \frac{1}{g^2} \text{Tr} \left\{ (\mathcal{P}_\mu a_\nu) [a^\mu, a^\nu] + \frac{1}{2} \bar{\varphi} \Gamma^\mu [a_\mu, \varphi] + (\mathcal{P}_\mu b) [a^\mu, c] \right\} \\ &- \frac{1}{4g^2} \text{Tr} [a_\mu, a_\nu]^2, \end{aligned} \quad (2.3)$$

where $\mathcal{P}_\mu \equiv [P_\mu, \cdot]$, $F_{\mu\nu} \equiv i[P_\mu, P_\nu]$ and $\mathcal{F}_{\mu\nu} \equiv [F_{\mu\nu}, \cdot]$. If the background is not a classical solution, e.g. fuzzy sphere or fuzzy torus, the $O(a_\mu)$ term does not vanish.

2.1 IIB matrix model on fuzzy T^2 background

First, we introduce the $N \times N$ clock and shift matrices U and V :

$$U = \begin{pmatrix} 1 & & & \\ & e^{2\pi i/N} & & \\ & & e^{2 \cdot 2\pi i/N} & \\ & & & \ddots \end{pmatrix}, \quad V = \begin{pmatrix} 0 & & & 1 \\ 1 & 0 & & \\ & \ddots & \ddots & \\ & & & 1 & 0 \end{pmatrix}, \quad (2.4)$$

where U and V satisfy

$$UV = e^{2\pi i/N} VU, \quad U^n V^m = e^{2\pi i n m / N} V^m U^n, \quad (2.5)$$

$$\text{Tr} U^n = \text{Tr} V^n = 0 \quad (n = 1, \dots, N-1), \quad U^N = V^N = \mathbf{1}_N. \quad (2.6)$$

Using them, we construct a 2-dimensional fuzzy torus as follows :

$$\begin{aligned}
P_1 + iP_2 &= 2\sqrt{N}L_1U, & P_1 - iP_2 &= 2\sqrt{N}L_1U^{-1}, \\
P_3 + iP_4 &= 2\sqrt{N}L_2V, & P_3 - iP_4 &= 2\sqrt{N}L_2V^{-1}, \\
P_1 &= \sqrt{N}L_1(U + U^{-1}), & P_2 &= -i\sqrt{N}L_1(U - U^{-1}), \\
P_3 &= \sqrt{N}L_2(V + V^{-1}), & P_4 &= -i\sqrt{N}L_2(V - V^{-1}), \\
P_5 &= \dots = P_{10} = 0.
\end{aligned} \tag{2.7}$$

Here, L_1 and L_2 are the noncommutativity parameters, which have the dimension² of mass. Their product, $L^2 = L_1L_2$, corresponds to the noncommutativity parameter B of fuzzy plane. The relation of this background to fuzzy plane is discussed more precisely in section 2.4.

We can expand the fluctuations in terms of U and V . For example, a_μ can be expressed as

$$a_\mu = \sum_{m_1, m_2=1}^N \tilde{a}_\mu(m_1, m_2) U^{m_2} V^{-m_1}, \tag{2.8}$$

and the hermiticity condition is given by

$$\tilde{a}_\mu^*(m_1, m_2) = e^{-2\pi i m_1 m_2 / N} \tilde{a}_\mu(-m_1, -m_2). \tag{2.9}$$

We will show that this expansion corresponds to the ordinary Fourier expansion in section 2.4. Using these Fourier modes, we can construct the Feynman rules, which we summarize in Appendix A.

2.2 IIB matrix model on fuzzy T^4 background

We can similarly construct fuzzy T^4 using the tensor products of the fuzzy tori constructed above :

$$\begin{aligned}
P_1 &= \sqrt{N_1}L_1(U_1 + U_1^{-1}) \otimes \mathbf{1}_{N_2}, & P_2 &= -i\sqrt{N_1}L_1(U_1 - U_1^{-1}) \otimes \mathbf{1}_{N_2}, \\
P_3 &= \sqrt{N_1}L_1(V_1 + V_1^{-1}) \otimes \mathbf{1}_{N_2}, & P_4 &= -i\sqrt{N_1}L_1(V_1 - V_1^{-1}) \otimes \mathbf{1}_{N_2}, \\
P_5 &= \sqrt{N_2}L_2 \mathbf{1}_{N_1} \otimes (U_2 + U_2^{-1}), & P_6 &= -i\sqrt{N_2}L_2 \mathbf{1}_{N_1} \otimes (U_2 - U_2^{-1}), \\
P_7 &= \sqrt{N_2}L_2 \mathbf{1}_{N_1} \otimes (V_2 + V_2^{-1}), & P_8 &= -i\sqrt{N_2}L_2 \mathbf{1}_{N_1} \otimes (V_2 - V_2^{-1}), \\
P_9 &= P_{10} = 0.
\end{aligned} \tag{2.10}$$

Here, $N = N_1N_2$, and U_i, V_i are the $N_i \times N_i$ clock and shift matrices. For simplicity, we set the radii of the two circles in the first T^2 to the same value $2\sqrt{N_1}L_1$, and similarly in the second T^2 to $2\sqrt{N_2}L_2$. In the following sections, we first fix the value of N , and calculate the free energy as a function of $R = \frac{N_2}{N_1}$, $L = \sqrt{L_1L_2}$ and $r = \frac{L_2}{L_1}$, and minimize it with respect to them.

2.3 k -coincident fuzzy tori

We also consider a system of k -coincident fuzzy tori. To study k -coincident fuzzy T^2 , we replace $U_{(N)}$ and $V_{(N)}$ with $U_{(N/k)} \otimes \mathbf{1}_k$ and $V_{(N/k)} \otimes \mathbf{1}_k$, where $U_{(N)}$ and $V_{(N)}$ stand for the $N \times N$ clock and shift matrices, respectively. Then, the Fourier modes $\tilde{a}_\mu, \tilde{\varphi}, \tilde{b}$ and \tilde{c} become $k \times k$ matrices.

Similarly, in the case of fuzzy T^4 , we can replace $U_1 \otimes \mathbf{1}_{N_2}$ with $U_1 \otimes \mathbf{1}_{N_2} \otimes \mathbf{1}_k$, and so on, to construct a k -coincident T^4 . In this case, we have $N = N_1N_2k$.

²In IIB matrix model, usually we treat A_μ as the spacetime coordinate. However, when we map IIB matrix model to the non-commutative Yang-Mills theory, we usually regard P_μ as the momentum operator and assign the mass dimension to A_μ .

2.4 Correspondence between fuzzy torus and flat fuzzy space

In this section, we discuss the relation between the fuzzy torus and flat fuzzy space [11]. To be specific, we consider the case of fuzzy T^2 and flat fuzzy plane (flat D1-brane). Generalization to higher dimensions is straightforward.

In order to avoid confusion, we denote fuzzy plane background as Q_μ and that of fuzzy torus as P_μ . The fuzzy plane is characterized by the constant commutators :

$$[Q_1, Q_2] = -iB, \quad Q_3 = \dots = Q_{10} = 0. \quad (2.11)$$

Let us write U and V as

$$U = \exp\left(i\sqrt{\frac{2\pi}{NB}}Q'_1\right), \quad V = \exp\left(i\sqrt{\frac{2\pi}{NB}}Q'_2\right). \quad (2.12)$$

Then, if we consider the region where eigenvalues of Q'_1 and Q'_2 are close to zero, the condition $UV = e^{2\pi i/N}VU$ is equivalent to $[Q'_1, Q'_2] = -iB$. Therefore, $Q_i \simeq Q'_i$ in this region. On the other hand, if we compare (2.7) with

$$Q'_1 \simeq -\frac{i}{2}\sqrt{\frac{NB}{2\pi}}(U - U^{-1}), \quad Q'_2 \simeq -\frac{i}{2}\sqrt{\frac{NB}{2\pi}}(V - V^{-1}), \quad (2.13)$$

we have the identifications in the embedded space as $P_2 \simeq \text{const.}Q'_1, P_4 \simeq \text{const.}Q'_2$. In general, tangent spaces of fuzzy torus look like fuzzy planes.

IIB matrix model on fuzzy torus can be mapped to NCSYM as in the case of flat fuzzy space [6, 11]. If we introduce the spacetime coordinates as

$$\hat{x}_1 = -\frac{Q_2}{B}, \quad \hat{x}_2 = \frac{Q_1}{B}, \quad (2.14)$$

we have

$$\begin{aligned} U^{m_2}V^{-m_1} &\sim e^{-im_2\sqrt{\frac{2\pi B}{N}}\hat{x}_2}e^{-im_1\sqrt{\frac{2\pi B}{N}}\hat{x}_1} \\ &= e^{i\sum_i k_i \hat{x}_i} \times (\text{phase}), \end{aligned} \quad (2.15)$$

where momenta k_i are defined by $k_i = m_i\sqrt{\frac{2\pi B}{N}}$. Hence the expansion(2.8) becomes the ordinary Fourier expansion in the commutative limit.

3 Calculation of free energy

We calculate the free energies in this section. We ignore the tachyons and zero modes on the fuzzy torus in our calculations. The vector- and fermion-kinetic terms on fuzzy torus have tachyons and extra zero-modes besides those coming from the U(1)-part. (See Appendix D for the detail.) Therefore, it is not clear whether perturbative calculation is possible or not. However, the number of tachyons remains the same in the large- N limit, and their mass squared is of $O\left(\frac{1}{N}\right)$ and vanishes in the large- N limit. Hence we expect that the tachyons give a relative correction of $O\left(\frac{\log(N)}{N^2}\right)$ to the free energy.

On the other hand, in the case of T^4 and $N_1 \sim N_2 \sim \sqrt{N}$, we will see that the leading contributions cancel out due to the supersymmetry, but the terms of $O\left(\frac{1}{N}\right)$ do not vanish. They are expected to be larger than the effect of the tachyons, and we can take the large- N limit without paying much attention to the tachyons.

3.1 Tree-level free energy

We start with the tree-level free energy. It is given by

$$\begin{aligned}
-\frac{1}{4g^2} \sum_{i,j} \text{Tr} [P_i, P_j]^2 &= \frac{16L^2 N^3}{g^2} \sin^2 \left(\frac{\pi}{N} \right) \\
&\rightarrow \frac{16N\pi^2 L^2}{g^2} \quad (\text{in the large-}N \text{ limit})
\end{aligned} \tag{3.1}$$

for T^2 , and

$$\begin{aligned}
-\frac{1}{4g^2} \sum_{i,j} \text{Tr} [P_i, P_j]^2 &= \frac{16L^2 N^3}{g^2} \sin^2 \left(\frac{\pi}{N} \right) \left(r^2 + \frac{1}{r^2} \right) \\
&\rightarrow \frac{16N\pi^2 L^2}{g^2} \left(r^2 + \frac{1}{r^2} \right) \quad (\text{in the large-}N \text{ limit})
\end{aligned} \tag{3.2}$$

for T^4 , respectively.

3.2 1-loop free energy

The 1-loop free energy can be easily evaluated as [1]

$$-\frac{1}{2} \sum_{n=1}^{\infty} \frac{1}{n} \text{Tr} \left(-\frac{2i}{\mathcal{P}^2} \mathcal{F}_{ij} \right)^n + \frac{1}{4} \sum_{n=1}^{\infty} \frac{1}{n} \text{Tr} \left(\frac{i}{2\mathcal{P}^2} \mathcal{F}_{ij} \gamma^{ij} \right)^n. \tag{3.3}$$

The terms for $n = 1, 2, 3$ cancel out, and the first nonzero contribution comes from $n = 4$. In the case of T^4 and $N_1 \sim N_2 \sim \sqrt{N}$, it is $O(N^0)$ and can be neglected compared with the tree-level and 2-loop level contributions. In the case of T^2 , truncation at some order of \mathcal{F} is not a good approximation because of infrared divergence.

Instead, we can numerically evaluate the 1-loop free energy without expanding in \mathcal{F} . We calculate all the eigenvalues of the kinetic terms, and sum up their logarithms. We find that the 1-loop free energy on T^2 background is proportional to $\log N$ and hence negligible compared to the tree level and 2-loop contributions. ³

3.3 2-loop free energy

Next we evaluate the 2-loop free energy on the fuzzy T^4 . Since it is difficult to obtain analytic forms of the vector and fermion propagators, we expand them in powers of \mathcal{F} as shown in Appendix A.1, and calculate the free energy order by order in \mathcal{F} . A naive power counting shows that each power of \mathcal{F} is associated with $\frac{1}{N}$ and $\frac{1}{\sqrt{N}}$ for T^2 and T^4 , respectively, if there is no infrared divergence. In fact, this expansion is good on the T^4 background, while it is not on the T^2 background. We discuss the validity of this expansion in Appendix C. Here we show the result for the T^4 background.

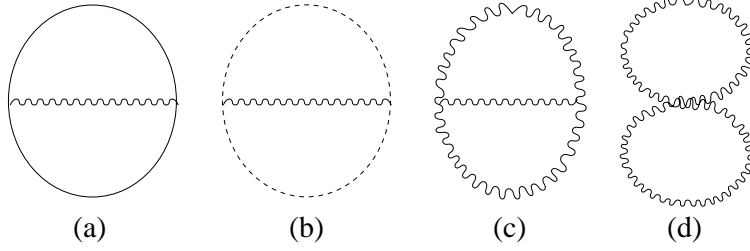


Figure 1: 2-loop vacuum diagrams

3.3.1 $O(\mathcal{F}^0)$

We have four kinds of 1PI 2-loop vacuum diagrams (see Fig.1), and their contributions can be approximated as (see Appendix E for the detail)

$$(a) \rightarrow \frac{g^2}{8N^2L^4} \sum_{m,n} \frac{1 - \cos(2\pi m \circ n)}{F(m)^2 \cdot F(n)^2}, \quad (3.4)$$

$$(b) \rightarrow -\frac{g^2}{512N^2L^4} \sum_{m,n} \frac{1 - \cos(2\pi m \circ n)}{F(m)^2 \cdot F(n)^2}, \quad (3.5)$$

$$(c) \rightarrow \frac{27g^2}{512N^2} \sum_{m,n} \frac{1 - \cos(2\pi m \circ n)}{F(m)^2 \cdot F(n)^2}, \quad (3.6)$$

$$(d) \rightarrow -\frac{45g^2}{256N^2} \sum_{m,n} \frac{1 - \cos(2\pi m \circ n)}{F(m)^2 \cdot F(n)^2}. \quad (3.7)$$

where $m \circ n = m_\mu C^{\mu\nu} n_\nu = \frac{m_1 n_2 - m_2 n_1}{N_1} + \frac{m_3 n_4 - m_4 n_3}{N_2}$, and $F(n)^2 = \sum_j F_j(n) \cdot F_j(n)$. $F_j(n)$ are analogous to the ordinary momentum variables in the continuum limit and given in appendix E .

Summing up these approximated values (3.4)~(3.7), we have

$$\left(\frac{1}{8} - \frac{1}{512} + \frac{27}{512} - \frac{45}{256} \right) \frac{g^2}{N^2} \sum_{m,n} \frac{1 - \cos(2\pi m \circ n)}{F(m)^2 \cdot F(n)^2} = 0. \quad (3.8)$$

This cancellation is not exact, but we can see numerically that the exact contribution of $O(\mathcal{F}^0)$ terms is smaller than that of $O(\mathcal{F}^2)$ terms.

3.3.2 $O(\mathcal{F}^1)$

The $O(\mathcal{F}^1)$ contribution is zero, because integrands are odd function of the momenta.

3.3.3 $O(\mathcal{F}^2)$

The calculation of $O(\mathcal{F}^2)$ contribution is very tedious. Here we show only the simplest case, that is, the planar part of Fig.1 (b). In this case, the contribution can be written as

$$\frac{g^2 N}{L^4} f_b(R, r), \quad (3.9)$$

³In this calculation, we have discarded the tachyons and the extra zero-modes.

where

$$\begin{aligned}
& f_b(R, r) \\
&= \frac{\pi^2}{256} \int d^4k d^4l \left\{ \frac{1 - \cos(2\pi(k_1 + l_1)) \cos(2\pi(k_2 + l_2))}{F(k)^2 \cdot F(l)^2 \cdot (F(k+l)^2)^3} \right. \\
&\times \frac{1}{r^3 \sqrt{R}} (\sin(\pi k_1) \sin(\pi l_1) \cos(\pi(k_1 + l_1)) + \sin(\pi k_2) \sin(\pi l_2) \cos(\pi(k_2 + l_2))) \\
&+ \frac{1 - \cos(2\pi(k_3 + l_3)) \cos(2\pi(k_4 + l_4))}{F(k)^2 \cdot F(l)^2 \cdot (F(k+l)^2)^3} \\
&\left. \times r^3 \sqrt{R} (\sin(\pi k_3) \sin(\pi l_3) \cos(\pi(k_3 + l_3)) + \sin(\pi k_4) \sin(\pi l_4) \cos(\pi(k_4 + l_4))) \right\}.
\end{aligned} \tag{3.10}$$

Here $k_i = m_i/N_1, k_j = m_j/N_2, l_i = n_i/N_1, l_j = n_j/N_2$ ($i = 1, 2; j = 3, 4$), and k_μ and l_μ vary from 0 to 1. Because the ghost propagators do not contain \mathcal{F} , this expression is rather simple. The contributions from the other diagrams (Fig.1 (a),(b),(c)) also can be written as $\frac{g^2 N}{L^4} f_a(R, r)$, $\frac{g^2 N}{L^4} f_c(R, r)$ and $\frac{g^2 N}{L^4} f_d(R, r)$. But the expressions of $f_a(R, r)$, $f_c(R, r)$ and $f_d(R, r)$ become much more complicated, because both vector and fermion propagators contain $O(\mathcal{F})$ corrections. Summing up all of the diagrams, we find that the leading behavior of the $O(\mathcal{F}^2)$ contribution can be expressed as

$$\frac{g^2 N}{L^4} \cdot h(R, r). \tag{3.11}$$

The function $h(R, r) = \sum_{j=a,b,c,d} f_j(R, r)$ is dimensionless and has a symmetry under the exchange of two tori

$$h(R, r) = h(R^{-1}, r^{-1}). \tag{3.12}$$

3.4 Total Free energy

The total free energy on the fuzzy T^4 background can be written as

$$\frac{16N\pi^2 L^4}{g^2} \left(r^2 + \frac{1}{r^2} \right) + \frac{g^2 N}{L^4} \cdot h(R, r) + O(g^4), \tag{3.13}$$

where we have neglected subleading terms in N . The $O(g^4)$ terms come from higher-loop diagrams. If we neglect them and minimize the free energy with respect to L , we obtain the minimum value

$$E(R, r; N) = 4\pi N \sqrt{\left(r^2 + \frac{1}{r^2} \right) h(R, r)} \tag{3.14}$$

at

$$\frac{L^4}{g^2} = \frac{1}{4\pi} \sqrt{\frac{h(R, r)}{\left(r^2 + \frac{1}{r^2} \right)}}. \tag{3.15}$$

The situation does not change qualitatively, even if we take the full order of the loop expansion into account. In general, the n -loop diagrams are proportional to $\left(\frac{g^2}{L^4}\right)^{n-1} N^2$. However, the $O(\mathcal{F}^0)$ contributions cancel due to the supersymmetry⁴, and the $O(\mathcal{F}^1)$ contributions vanish because they are given by integrals of odd functions. Therefore, if we include the contribution from the higher-loop diagrams, the free energy can be expressed as

$$N \sum_{j=0}^{\infty} \left(\frac{g^2}{L^4} \right)^{j-1} h_j(R, r), \tag{3.16}$$

where h_j are of $O(1)$. The minimum value is again of $O(N)$.

⁴See Appendix B for the detail.

3.5 The case of k -coincident fuzzy tori

Here we consider the system of k -coincident fuzzy tori. This system can be mapped to $U(k)$ NCSYM. The free energy in this case becomes

$$kN \sum_{j=0}^{\infty} \left(\frac{g^2 k}{L^4} \right)^{j-1} h_j(R, r). \quad (3.17)$$

Therefore, the single fuzzy torus has the lowest free energy, and $U(1)$ gauge group is favored in this case.

4 Numerical comparison of free energies

As the analytic expressions are very complicated, here we try to compare the free energies numerically. First, we consider $h(R, r)$. It is given by an 8-fold integral, and we have evaluated it approximately using the quadrature by parts.

We divide the integration domain into M bins in each direction, with $M = 9, 10, \dots, 15$. Let $h(R, r; M)$ be the value of $h(R, r)$ evaluated by M bins. We have fitted the plot of $h(R, r; M)$ versus $1/M$ by a polynomial, and estimated $h(R, r) = h(R, r; \infty)$ extrapolating it up to $1/M \rightarrow 0$. In Fig.2,

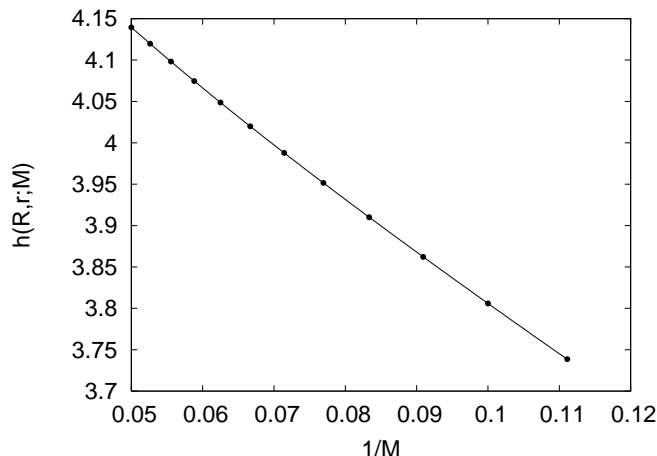


Figure 2: $h(R, r; M)$ versus $1/M$ for $R = r = 1$. The curve shows a nice polynomial fitting.

we plot $h(R, r; M)$ against $1/M$ for $R = 1$ and $r = 1$. The curve shows a nice polynomial fitting. We can evaluate the $h(R, r) = h(R, r; \infty)$ replacing $1/M = 0$ in the polynomial.

Once we have $h(R, r)$, we can readily obtain $E(R, r; N)$ from eqn. (3.14). We plot $E(R = 1, r; N)/N$ as a function of r for R fixed to 1 in Fig.3. We see that $R = r = 1$ is the minimum. Therefore, the fuzzy T^4 is favored under the variation of the ratio r of the noncommutativity.

Fig.4 shows $E(R, r = 1; N)/N$ as a function of R for r fixed to 1, and this time $R = r = 1$ is the maximum. Therefore, we find that the fuzzy T^4 is *unstable* under the variation of the ratio R of the matrix sizes.

To compare with the result for the fuzzy $S^2 \times S^2$ in [9], we plot $E(R, r = \sqrt{R}; N)/N$ as a function of r in Fig.5. The curve $r = \sqrt{R}$ is the same as the one studied for the fuzzy $S^2 \times S^2$ in [9]. On this curve, $R = r = 1$ is the minimum, hence the fuzzy T^4 is favored. This observation is similar to the fuzzy $S^2 \times S^2$. In [9], it is pointed out that although the 2-loop contribution ($h(R, r = \sqrt{R})$ in our notation) is maximum at $R = r = 1$, the tree-level contribution, $\sim r^2 + \frac{1}{r^2} = R + \frac{1}{R}$, is minimum at

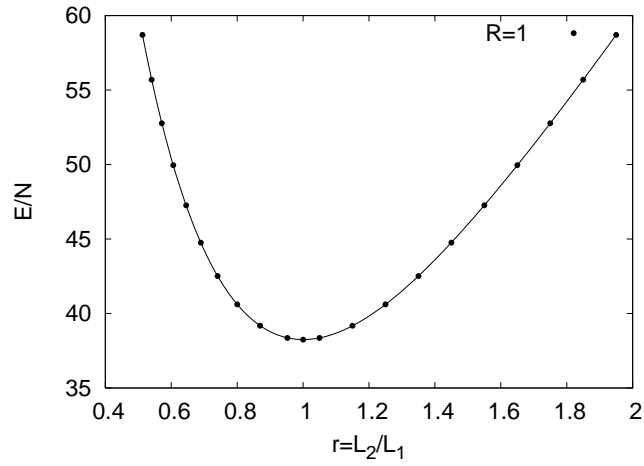


Figure 3: $E(R, r; N)/N$ against r for fixed $R = 1$. $R = r = 1$ is the minimum here. T^4 is favored under variation of r .

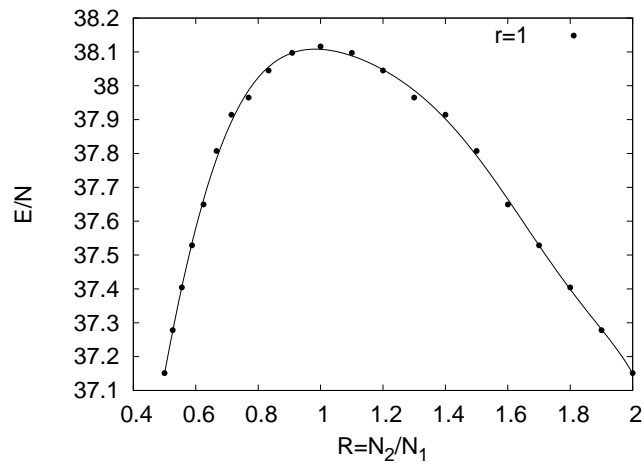


Figure 4: $E(R, r; N)/N$, against R for fixed $r = 1$. $R = r = 1$ is the maximum here. T^4 unstable under variation of R .

$R = r = 1$ and this makes the total free energy minimum at $R = r = 1$. We have exactly the same situation here.

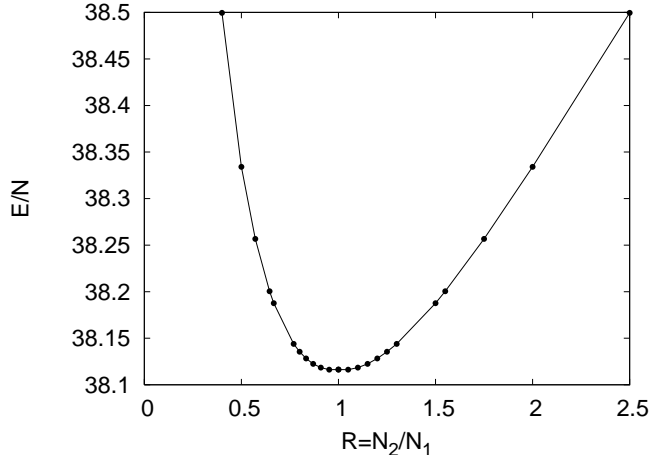


Figure 5: $E(R, r; N)/N$ against R for $R = r^2$. $R = r = 1$ is the minimum here. T^4 is favored.

These results show that although the fuzzy T^4 is favourable in some directions, it is unstable under the variation of R . Because the limit $R \rightarrow 0$ or ∞ corresponds to the fuzzy T^2 , we conclude that the fuzzy T^2 is more favourable than the fuzzy T^4 . Since our observations along $r = \sqrt{R}$ is completely analogous to that of [9], it is plausible that the fuzzy $S^2 \times S^2$ also has the same kind of instability. A similar phenomenon is observed in a 6 dimensional bosonic matrix model with Chern Simons term, where S^2 is indeed shown to be more favourable than $S^2 \times S^2$ [12].

We can compare the free energy of the fuzzy T^4 and the fuzzy $S^2 \times S^2$. At $R = r = 1$, the free energy of T^4 is $\simeq 38.1N$. According to [9], the free energy of $S^2 \times S^2$ with the same matrix size and noncommutativity is $\simeq 3.6N$. Therefore, $S^2 \times S^2$ is more favorable than T^4 .

We have also computed the 2-loop free energy of the fuzzy T^2 up to $O(\mathcal{F}^2)$ as a function of the ratio of radii, L_1/L_2 . We found that it has the minimum at $L_1 = L_2$ and is proportional to N . However, because the \mathcal{F} expansion is not good in this background, this result is not reliable. The free energy on the S^2 background is calculated in [10]. In this case, the tree-level action dominates and the free energy is 0 at $L = 0$.

5 Conclusions and discussions

In this paper, we have calculated the free energies of IIB matrix model on the fuzzy T^4 backgrounds up to 2-loop level. The free energy on T^4 is a function of the ratio r of the noncommutativity and R of the matrix size. At $R = r = 1$, the free energy takes minimum when r is varied, but maximum when R is varied. This indicates that T^2 is more stable than T^4 . It is plausible that $S^2 \times S^2$ has the same sort of instability. If so, a four-dimensional vacuum might not be realized as a direct product of two noncommutative surfaces. Commutative backgrounds seem to be more plausible. Another possibility is that new terms like Myers term arise dynamically (for example via large- N RG) and stabilize noncommutative spaces.

We also have compared the free energies of $S^2 \times S^2$ and T^4 , and found that the latter is about 10 times as large as the former. It implies that IIB matrix model favors configurations with higher symmetry.

Furthermore, we calculated the free energy of the system of k -coincident fuzzy T^4 , and found that the $k = 1$ system has the smallest free energy. In terms of NCSYM, this means that $U(1)$ gauge group

is favored. This result is the same as that of the fuzzy sphere in IIB matrix model [9] and in bosonic matrix models with Chern Simons term [13]. It seems that in general noncommutative backgrounds favor U(1) gauge group.

Acknowledgments

The authors would like to thank Y.Kimura, Y.Matsuo and A.Miwa for fruitful discussions. S.B. was supported in part by the Grants-in-Aid for Scientific Research (No. P02040) the Ministry of Education, Culture, Sports, Science and Technology of Japan. M.H. would like to thank the Japan Society for the Promotion of Science for financial support. This work was also supported in part by a Grant-in-Aid for the 21st Century COE “Center for Diversity and Universality in Physics”.

A Feynman rules of IIB matrix model on fuzzy T^2 background

In this section, we summarize the Feynman rules of IIB matrix model on the T^2 background. Generalization to the T^4 background is straightforward.

A.1 Propagators

Boson (vector and scalar)

The kinetic term for a_μ is given by

$$\begin{aligned} & \frac{1}{2g^2} \text{Tr} a_\mu \{ \mathcal{P}^2 \delta_{\mu\nu} - 2i\mathcal{F}_{\mu\nu} \} a_\nu \\ &= \frac{N}{2g^2} \sum_{m,n} e^{-2\pi i m_1 m_2 / N} \tilde{a}_\mu(-m_1, -m_2) \{ \mathcal{P}^2 \delta_{\mu\nu} - 2i\mathcal{F}_{\mu\nu} \}_{m_1 m_2; n_1 n_2} \tilde{a}_\nu(n_1, n_2), \end{aligned} \quad (\text{A.1})$$

and the propagator is expressed as

$$\langle \tilde{a}_\mu(-m_1, -m_2) \tilde{a}_\nu(n_1, n_2) \rangle = \frac{g^2}{N} \{ \mathcal{P}^2 \delta_{\mu\nu} - 2i\mathcal{F}_{\mu\nu} \}_{m_1 m_2; n_1 n_2}^{-1} \times e^{2\pi i n_1 n_2 / N}. \quad (\text{A.2})$$

We expand it with respect to \mathcal{F} and truncate it at some order :

$$\begin{aligned} & \{ \mathcal{P}^2 \delta_{\mu\nu} - 2i\mathcal{F}_{\mu\nu} \}^{-1} \\ &= \left\{ \frac{\delta_{\mu\nu}}{\mathcal{P}^2} + 2i \frac{1}{\mathcal{P}^2} \mathcal{F}_{\mu\nu} \frac{1}{\mathcal{P}^2} - 4 \frac{1}{\mathcal{P}^2} \mathcal{F}_{\mu\rho} \frac{1}{\mathcal{P}^2} \mathcal{F}_{\rho\nu} \frac{1}{\mathcal{P}^2} + \dots \right\}. \end{aligned} \quad (\text{A.3})$$

Note that this expansion is not good in this case but a similar expansion in the T^4 background is reliable.

Fermion

The fermion kinetic term is given by

$$-\frac{1}{2g^2} \text{Tr} \tilde{\varphi} \mathcal{P} \varphi = -\frac{N}{2g^2} \sum_{m,n} e^{-2\pi i m_1 m_2 / N} \varphi^T(-m_1, -m_2) \mathcal{P}_{m_1 m_2; n_1 n_2} \varphi(n_1, n_2), \quad (\text{A.4})$$

and the propagator is expressed as

$$\langle \tilde{\varphi}_i(-m_1, -m_2) \tilde{\varphi}_j(n_1, n_2) \rangle = \frac{g^2}{N} \left(\frac{1}{\mathcal{P}} \right)_{ij; m_1 m_2; n_1 n_2} \times e^{2\pi i n_1 n_2}. \quad (\text{A.5})$$

Here we also expand $\frac{1}{\mathcal{P}}$ in powers of \mathcal{F} :

$$\begin{aligned}\frac{1}{\mathcal{P}} &= \left\{ \mathcal{P}^2 + \frac{i}{2} \gamma^{\mu\nu} \mathcal{F}_{\mu\nu} \right\}^{-1} \mathcal{P} \\ &= \left\{ \frac{1}{\mathcal{P}^2} - \frac{i}{2} \frac{1}{\mathcal{P}^2} \gamma^{\mu\nu} \mathcal{F}_{\mu\nu} \frac{1}{\mathcal{P}^2} - \frac{1}{4} \frac{1}{\mathcal{P}^2} \gamma^{\mu\nu} \mathcal{F}_{\mu\nu} \frac{1}{\mathcal{P}^2} \gamma^{\rho\sigma} \mathcal{F}_{\rho\sigma} \frac{1}{\mathcal{P}^2} + \dots \right\} \mathcal{P}.\end{aligned}\tag{A.6}$$

Ghost

The Ghost kinetic term and propagator are given, respectively, by

$$\frac{1}{g^2} \text{Tr } b \mathcal{P}^2 c = \frac{N}{g^2} \sum_{m,n} e^{-2\pi i m_1 m_2 / N} \tilde{b}(-m_1, -m_2) (\mathcal{P}^2)_{m_1 m_2; n_1 n_2} \tilde{c}(n_1, n_2),\tag{A.7}$$

and

$$\langle \tilde{b}(-m_1, -m_2) \tilde{c}(n_1, n_2) \rangle = \frac{g^2}{N} (\mathcal{P}^2)_{m_1 m_2; n_1 n_2}^{-1} \times e^{2\pi i n_1 n_2 / N}.\tag{A.8}$$

A.2 Explicit form of \mathcal{P}

A direct calculation shows that

$$\begin{aligned}[P_1, a_\mu] &= -2i\sqrt{N}L_1 \sum_m U^{m_2} V^{-m_1} \sin\left(\frac{\pi m_1}{N}\right) \left\{ \tilde{a}_\mu(m_1, m_2 - 1) e^{\pi i m_1 / N} - \tilde{a}_\mu(m_1, m_2 + 1) e^{-\pi i m_1 / N} \right\}, \\ [P_2, a_\mu] &= -2\sqrt{N}L_1 \sum_m U^{m_2} V^{-m_1} \sin\left(\frac{\pi m_1}{N}\right) \left\{ \tilde{a}_\mu(m_1, m_2 - 1) e^{\pi i m_1 / N} + \tilde{a}_\mu(m_1, m_2 + 1) e^{-\pi i m_1 / N} \right\}, \\ [P_3, a_\mu] &= -2i\sqrt{N}L_2 \sum_m U^{m_2} V^{-m_1} \sin\left(\frac{\pi m_2}{N}\right) \left\{ \tilde{a}_\mu(m_1 + 1, m_2) e^{-\pi i m_2 / N} - \tilde{a}_\mu(m_1 - 1, m_2) e^{\pi i m_2 / N} \right\}, \\ [P_4, a_\mu] &= -2\sqrt{N}L_2 \sum_m U^{m_2} V^{-m_1} \sin\left(\frac{\pi m_2}{N}\right) \left\{ \tilde{a}_\mu(m_1 + 1, m_2) e^{-\pi i m_2 / N} + \tilde{a}_\mu(m_1 - 1, m_2) e^{\pi i m_2 / N} \right\}.\end{aligned}\tag{A.9}$$

From these equations, we obtain

$$(\mathcal{P}_1)_{m_1 m_2; n_1 n_2} = \begin{cases} \pm 2i\sqrt{N}L_1 \sin\left(\frac{\pi m_1}{N}\right) e^{\mp \pi i m_1 / N} & ((n_1, n_2) = (m_1, m_2 \pm 1)) \\ 0 & (\text{otherwise}) \end{cases},\tag{A.10}$$

and so on. This expression is not very simple, but \mathcal{P}^2 can be written in the following simple form :

$$(\mathcal{P}^2)_{m_1 m_2; n_1 n_2} = 16N \sum_i L_i^2 \sin^2\left(\frac{\pi m_i}{N}\right) \delta_{m_1 n_1} \delta_{m_2 n_2}.\tag{A.11}$$

A.3 Interaction vertices

There are four types of interaction vertices (Fig.6). Here, the solid, dotted and wavy lines represent the fermions, ghosts and bosons, respectively.

(a) Fermion-fermion-boson coupling V_{3f}

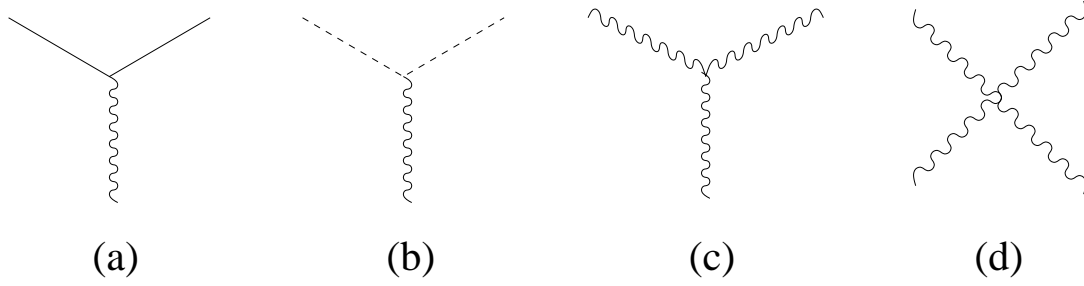


Figure 6: Interaction vertices

$$\begin{aligned}
V_{3f} &= -\frac{iN}{g^2} \sum_{k,l} \tilde{\varphi}_i(k) (\gamma^\mu)_{ij} \tilde{a}_\mu(-k-l) \tilde{\varphi}_j(l) e^{-\pi i \{k_1 k_2 + l_1 l_2 + (k_1 + l_1)(k_2 + l_2)\} / N} \sin(\pi k \circ l), \\
C^{ij} &\equiv \frac{1}{N} \begin{pmatrix} 0 & 1 \\ -1 & 0 \end{pmatrix}_{ij}, \quad k \circ l = \sum_{i,j} k_i C^{ij} l_j = \frac{k_1 l_2 - k_2 l_1}{N}.
\end{aligned} \tag{A.12}$$

Note that $\mu = 1, 2, \dots, 10$ (Both vectors and scalars couple to the fermion).

(b) Ghost-ghost-vector coupling V_{3g}

$$\begin{aligned}
V_{3g} &= 2i \frac{(2N)^{3/2}}{g^2} \sum_{m,n} e^{-\pi i \{m_1 m_2 + n_1 n_2 + (m_1 + n_1)(m_2 + n_2)\} / N} \tilde{b}(m) \tilde{c}(n) \\
&\times \left\{ L_1 \sin\left(\frac{\pi m_1}{N}\right) e^{-\pi i(m_1 + n_1)/N} \sin\left(\pi m \circ n - \frac{\pi n_1}{N}\right) \tilde{a}_{1+}(-m_1 - n_1, -m_2 - n_2 - 1) \right. \\
&+ L_1 \sin\left(\frac{\pi m_1}{N}\right) e^{\pi i(m_1 + n_1)/N} \sin\left(\pi m \circ n + \frac{\pi n_1}{N}\right) \tilde{a}_{1-}(-m_1 - n_1, -m_2 - n_2 + 1) \\
&- L_2 \sin\left(\frac{\pi m_2}{N}\right) e^{-\pi i(m_2 + n_2)/N} \sin\left(\pi m \circ n + \frac{\pi n_2}{N}\right) \tilde{a}_{2-}(-m_1 - n_1 - 1, -m_2 - n_2) \\
&\left. - L_2 \sin\left(\frac{\pi m_2}{N}\right) e^{\pi i(m_2 + n_2)/N} \sin\left(\pi m \circ n - \frac{\pi n_2}{N}\right) \tilde{a}_{2+}(-m_1 - n_1 + 1, -m_2 - n_2) \right\},
\end{aligned} \tag{A.13}$$

where

$$\tilde{a}_{1\pm} \equiv \frac{\pm i \tilde{a}_1 + \tilde{a}_2}{\sqrt{2}}, \quad \tilde{a}_{2\pm} \equiv \frac{\mp i \tilde{a}_3 + \tilde{a}_4}{\sqrt{2}}. \tag{A.14}$$

Note that only vectors couple to the ghosts and scalars do not.

(c) Boson-boson-vector coupling V_{3b}

$$\begin{aligned}
V_{3b} &= 2i \frac{(2N)^{3/2}}{g^2} \sum_{m,n} e^{-\pi i \{m_1 m_2 + n_1 n_2 + (m_1 + n_1)(m_2 + n_2)\}/N} \tilde{a}_\mu(m) \tilde{a}^\mu(n) \\
&\times \left\{ L_1 \sin\left(\frac{\pi m_1}{N}\right) e^{-\pi i(m_1 + n_1)/N} \sin(\pi m \circ n - \pi n_1/N) \tilde{a}_{1+}(-m_1 - n_1, -m_2 - n_2 - 1) \right. \\
&\quad + L_1 \sin\left(\frac{\pi m_1}{N}\right) e^{\pi i(m_1 + n_1)/N} \sin(\pi m \circ n + \pi n_1/N) \tilde{a}_{1-}(-m_1 - n_1, -m_2 - n_2 + 1) \\
&\quad - L_2 \sin\left(\frac{\pi m_2}{N}\right) e^{-\pi i(m_2 + n_2)/N} \sin(\pi m \circ n + \pi n_2/N) \tilde{a}_{2-}(-m_1 - n_1 - 1, -m_2 - n_2) \\
&\quad \left. - L_2 \sin\left(\frac{\pi m_2}{N}\right) e^{\pi i(m_2 + n_2)/N} \sin(\pi m \circ n - \pi n_2/N) \tilde{a}_{2+}(-m_1 - n_1 + 1, -m_2 - n_2) \right\}. \tag{A.15}
\end{aligned}$$

(d) four-boson coupling V_{4b}

$$\begin{aligned}
V_{4b} &= \frac{N}{4g^2} \sum_{k,l,m,n} \tilde{a}_\mu(k) \tilde{a}_\nu(l) \tilde{a}_\mu(m) \tilde{a}_\nu(n) \delta_{k+l+m+n,0}^2 e^{-\pi i(k_1 k_2 + l_1 l_2 + m_1 m_2 + n_1 n_2)} \\
&\times \left\{ e^{\frac{\pi i}{2}(kol+lom+mon+nok)} + e^{-\frac{\pi i}{2}(kol+lom+mon+nok)} \right. \\
&\quad \left. - e^{\frac{\pi i}{2}(kol+lom+nok)} - e^{-\frac{\pi i}{2}(kol+lom+nok)} \right\}. \tag{A.16}
\end{aligned}$$

B Cancellation of free energy on torus background due to SUSY at $O(\mathcal{F}^0)$

First, we consider the cancellation of the free energy on flat fuzzy space backgrounds. On this background, the free energy should be zero at least formally. (The meaning of the word ‘‘formally’’ is explained shortly.)

For example, the sum of the two-loop diagrams is proportional to [10]

$$\int dk dl \left\{ \frac{1}{k^2 \cdot l^2} + \frac{2k \cdot l}{k^2 \cdot l^2 \cdot (k+l)^2} \right\}. \tag{B.1}$$

Naively this is zero, because $2k \cdot l = (k+l)^2 - k^2 - l^2$. However, if the size N of the matrices is finite, there should be some momentum cutoff, and (B.1) is not necessarily zero. For example, in the region where k and l are allowed but $k+l$ is outside the cutoff, the second term of (B.1) does not make sense. However, such problem occurs only in the large-momentum region. On the other hand in the small-momentum region, the free energy vanishes due to the supersymmetry. Therefore, it is natural to expect that the free energy is ‘‘formally’’ zero at any order of the loop expansion, if we use $2k \cdot l = (k+l)^2 - k^2 - l^2$ and shift the integration momentum not taking into account the cutoff. We assume this property.

Next, we consider the fuzzy torus background. Note that in this case the cutoff procedure is completely determined and there is no ambiguity. To be concrete, we consider the T^2 -background here. If we use the approximations such as $\tilde{a}_\mu(m_1, m_2 \pm 1) \simeq \tilde{a}_\mu(m_1, m_2)$, we have

$$\mathcal{P}_i \tilde{a}_\mu(m) = 4\sqrt{N} f_i(m) \tilde{a}_\mu(m), \tag{B.2}$$

where

$$\begin{aligned}
f_1(m) &\equiv L_1 \sin^2\left(\frac{\pi m_1}{N}\right), \\
f_2(m) &\equiv -L_1 \sin\left(\frac{\pi m_1}{N}\right) \cos\left(\frac{\pi m_1}{N}\right), \\
f_3(m) &\equiv -L_2 \sin^2\left(\frac{\pi m_2}{N}\right), \\
f_4(m) &\equiv -L_2 \sin\left(\frac{\pi m_2}{N}\right) \cos\left(\frac{\pi m_2}{N}\right).
\end{aligned} \tag{B.3}$$

Under this approximation, at $O(\mathcal{F}^0)$, the only difference from fuzzy plane is that the momentum $\frac{\pi m_i}{N}$ is replaced with $f_j(m)$.

The $f_j(m)$'s satisfy the following set of equations :

$$f^2(m) = \sum_i L_i^2 \sin^2\left(\frac{\pi m_i}{N}\right), \tag{B.4}$$

$$2f(m) \cdot f(-n) = f^2(m) + f^2(n) - f^2(m+n), \tag{B.5}$$

which is an analogue of $-2k \cdot l = k^2 + l^2 - (k+l)^2$. Using this, we can express the free energy only by $f^2(m)$'s. Since the momentum space is completely periodic in the fuzzy torus background, we can shift the integration variables without any obstruction, and find that the free energy is zero at this level. If we evaluate the free energy without using the approximations, there appear $O\left(\frac{1}{N}\right)$ -corrections.

C Validity of \mathcal{F} -expansion

In this section, we discuss the validity of the \mathcal{F} -expansion. First we consider the case of T^4 . \mathcal{F} 's are expressed in the momentum basis such as

$$\begin{aligned}
&(\mathcal{F}_{1+,2+})_{m_1-1,m_2-1,m_3,m_4;m_1,m_2,m_3,m_4} \\
&= -8i \sin\left(\frac{\pi}{N_1}\right) e^{\pi i/N_1} N_1 L_1^2 e^{-\pi i(m_1+m_2)/N_1} \sin\left(\frac{\pi(m_1-m_2)}{N_1}\right) \\
&\sim \sin\left(\frac{\pi(m_1-m_2)}{N_1}\right),
\end{aligned} \tag{C.1}$$

and \mathcal{P}^2 is expressed as

$$\begin{aligned}
&(\mathcal{P}^2)_{m_1,m_2,m_3,m_4;n_1,n_2,n_3,n_4} \\
&= 16 \left\{ \sum_{i=1,2} N_i L_i^2 \sin^2\left(\frac{\pi m_i}{N_i}\right) + \sum_{i=3,4} N_i L_i^2 \sin^2\left(\frac{\pi m_i}{N_i}\right) \right\} \delta_{mn}^4.
\end{aligned} \tag{C.2}$$

Hence, in the generic region, where $\frac{m_i}{N_i} = O(1)$ etc, one $\frac{1}{\mathcal{P}^2}\mathcal{F}$ -insertion amounts to multiplying $\frac{1}{N_1+N_2} \lesssim \frac{1}{\sqrt{N}}$.

However, if the arguments in sin are small, the situation changes. For example, if we take $N_1 \sim N_2 \sim \sqrt{N}$ and consider the region where all arguments in sin are of $O(N^{-\alpha})$ ($0 < \alpha \leq \frac{1}{2}$), then $\frac{1}{\mathcal{P}^2}\mathcal{F} \sim N^{\alpha-1/2}$. This shows that in the IR region convergence of the \mathcal{F} -expansion becomes worse. In the case that $N_1 \sim N_2 \sim \sqrt{N}$, the free energy does not have IR divergence. Therefore the generic region dominates, and the convergence of this expansion is good. Indeed, from the numerical calculations of the 2-loop free energy, we can see that one insertion of $\frac{1}{\mathcal{P}^2}\mathcal{F}$ decreases the power of N by $\frac{1}{2}$. On the other hand, in the case of T^2 background, the free energy has IR divergence. Therefore IR region dominates and the insertion of $\frac{1}{\mathcal{P}^2}\mathcal{F}$ does not decrease the power of N . In this case \mathcal{F} -expansion is not reliable.

D Tree-level tachyons and extra zero modes

On fuzzy torus, there exist zero and tachyonic modes, which we list below.

D.1 fermion zero modes

To be concrete we discuss the T^2 -case here. We use the following 4-dimensional gamma matrices:

$$\gamma^\mu = i \begin{pmatrix} 0 & -\sigma^{\mu\dagger} \\ \sigma^\mu & 0 \end{pmatrix}, \quad (\text{D.1})$$

where $\sigma^i (i = 1, 2, 3)$ are the Pauli matrices and $\sigma^4 = i \cdot \mathbf{1}_2$.

For the left-handed spinor, the Dirac operator is given by

$$\begin{aligned} \sigma^\mu \mathcal{P}_\mu &= \frac{\sigma^1 + i\sigma^2}{2} (\mathcal{P}_1 - i\mathcal{P}_2) + \frac{\sigma^1 - i\sigma^2}{2} (\mathcal{P}_1 + i\mathcal{P}_2) \\ &\quad + \frac{\sigma^3 + i\sigma^4}{2} (\mathcal{P}_3 - i\mathcal{P}_4) + \frac{\sigma^3 - i\sigma^4}{2} (\mathcal{P}_3 + i\mathcal{P}_4) \\ &= 2\sqrt{N} \begin{pmatrix} L_2[V, \cdot] & L_1[U^{-1}, \cdot] \\ L_1[U, \cdot] & -L_2[V^{-1}, \cdot] \end{pmatrix}. \end{aligned} \quad (\text{D.2})$$

Hence, there are two left-handed zero modes,

$$\begin{pmatrix} L_2V^{-1} \\ -L_1U \end{pmatrix} \quad \text{and} \quad \begin{pmatrix} L_1U^{-1} \\ L_2V \end{pmatrix}. \quad (\text{D.3})$$

Similarly for the right-handed spinors we have two zero modes given by

$$\begin{pmatrix} L_2V \\ -L_1U \end{pmatrix} \quad \text{and} \quad \begin{pmatrix} L_1U^{-1} \\ L_2V^{-1} \end{pmatrix}. \quad (\text{D.4})$$

These zero-modes are not doublers, because their momenta become zero in the large- N limit.

D.2 Zero and tachyonic modes of the vector

Although the numbers of zero and tachyonic modes depend on N , they become constant when N is sufficiently large. If the ratio $r = \frac{L_2}{L_1} = 1$, there are 4 zero modes and 5 tachyons. On the other hand, if $r \neq 1$, there are no zero modes and 7 tachyons.

A direct calculation shows that if $r = 1$, $(P_1, P_2, -P_3, -P_4)$ is an eigenstate with the smallest eigenvalue $-16NL^2 \sin^2\left(\frac{\pi}{N}\right)$. This mode corresponds to the deformation of the ratio r .

E 2-loop free energy : $O(\mathcal{F}^0)$ and $O(\mathcal{F}^2)$ contributions

Here we evaluate the $O(\mathcal{F}^0)$ and $O(\mathcal{F}^2)$ contributions to the 2-loop free energy on the fuzzy T^4 . For brevity of notation, we introduce the following notations

$$\begin{aligned} F_1(m) &\equiv \frac{1}{A} \sin^2\left(\frac{\pi m_1}{N}\right), & F_2(m) &\equiv -\frac{1}{A} \sin\left(\frac{\pi m_1}{N}\right) \cos\left(\frac{\pi m_1}{N}\right), \\ F_3(m) &\equiv -\frac{1}{A} \sin^2\left(\frac{\pi m_2}{N}\right), & F_4(m) &\equiv \frac{1}{A} \sin\left(\frac{\pi m_2}{N}\right) \cos\left(\frac{\pi m_2}{N}\right), \\ F_5(m) &\equiv A \sin^2\left(\frac{\pi m_3}{N}\right), & F_6(m) &\equiv -A \sin\left(\frac{\pi m_3}{N}\right) \cos\left(\frac{\pi m_3}{N}\right), \\ F_7(m) &\equiv -A \sin^2\left(\frac{\pi m_4}{N}\right), & F_8(m) &\equiv A \sin\left(\frac{\pi m_4}{N}\right) \cos\left(\frac{\pi m_4}{N}\right), \end{aligned}$$

where $A = \sqrt{r\sqrt{R}}$. We further introduce the abbreviation $F(m) \cdot F(n) = \sum_j F_j(m)F_j(n)$, which is the analogue of the inner product of momenta.

E.1 $O(\mathcal{F}^0)$

We have four kinds of 1PI 2-loop vacuum diagrams (Fig 1). We list the contributions from each diagram :

(a) Diagram with two fermion-fermion-boson vertices V_{3f}

$$\begin{aligned} & \frac{g^2}{4N^2L^4} \sum_{m,n} \frac{F(m) \cdot F(-n)}{F(m)^2 \cdot F(n)^2 \cdot F(m+n)^2} (1 - \cos(2\pi m \circ n)) \\ &= \frac{g^2}{8N^2L^4} \sum_{m,n} \frac{1}{F(m)^2 \cdot F(n)^2} (1 - \cos(2\pi m \circ n)). \end{aligned} \quad (\text{E.1})$$

Here we have used $2F(m) \cdot F(-n) = F(m)^2 + F(n)^2 + F(m+n)^2$.

(b) Diagram with two ghost-ghost-vector vertices V_{3g}

The exact result is given by

$$\begin{aligned} & -\frac{g^2}{512N^2L^4} \sum_{\pm} \sum_{m,n} \left\{ \frac{L_1^2 \sin\left(\frac{\pi m_2}{N_1}\right) \sin\left(\frac{\pi n_2}{N_1}\right)}{F(m_1 + n_1 \pm 1, m_2 + n_2, m_3 + n_3, m_4 + n_4)^2 \cdot F(m)^2 \cdot F(n)^2} \right. \\ & \quad \times \left\{ \cos\left(2\pi m \circ n \pm \pi \frac{n_2 - m_2}{N_1}\right) - \cos\left(\pi \frac{m_2 + n_2}{N_1}\right) \right\} \\ & \quad + \frac{L_1^2 \sin\left(\frac{\pi m_1}{N_1}\right) \sin\left(\frac{\pi n_1}{N_1}\right)}{F(m_1 + n_1, m_2 + n_2 \pm 1, m_3 + n_3, m_4 + n_4)^2 \cdot F(m)^2 \cdot F(n)^2} \\ & \quad \times \left\{ \cos\left(2\pi m \circ n \mp \pi \frac{n_1 - m_1}{N_1}\right) - \cos\left(\pi \frac{m_1 + n_1}{N_1}\right) \right\} \left. \right\} \\ & + (L_1, N_1, m_1, m_2, n_1, n_2 \leftrightarrow L_2, N_2, m_3, m_4, n_3, n_4). \end{aligned} \quad (\text{E.2})$$

Shifting m_i 's and introducing approximations,

$$\frac{1}{F(m_1 + n_1 \pm 1, m_2 + n_2, m_3 + n_3, m_4 + n_4)^2} \simeq \frac{1}{F(m_1 + n_1, m_2 + n_2, m_3 + n_3, m_4 + n_4)^2} \quad (\text{E.3})$$

and so on, we obtain

$$-\frac{g^2}{512N^2L^4} \sum_{m,n} \frac{1 - \cos(2\pi m \circ n)}{F(m)^2 \cdot F(n)^2}. \quad (\text{E.4})$$

(c) Diagram with two boson-boson-vector vertices V_{3b}

The exact result is given by

$$\begin{aligned}
& \frac{9g^2 L_1^2}{512N^2} \sum_{\pm} \sum_{m,n} \frac{1}{F(m_1 + n_1 \mp 1, m_2 + n_2, m_3 + n_3, m_4 + n_4)^2 \cdot F(m)^2 \cdot F(n)^2} \\
& \quad \times \left\{ \sin^2 \left(\frac{\pi m_2}{N_1} \right) \left\{ 1 - \cos \left(2\pi m \circ n \mp \frac{2\pi n_2}{N_1} \right) \right\} \right. \\
& \quad \quad \left. - \sin \left(\frac{\pi m_2}{N_1} \right) \sin \left(\frac{\pi n_2}{N_1} \right) \left\{ \cos \left(\frac{\pi(m_2 + n_2)}{N_1} \right) - \cos \left(2\pi m \circ n \pm \frac{\pi(m_2 - n_2)}{N_1} \right) \right\} \right\} \\
& + \frac{9g^2 L_1^2}{512N^2} \sum_{\pm} \sum_{m,n} \frac{1}{F(m_1 + n_1, m_2 + n_2 \pm 1, m_3 + n_3, m_4 + n_4)^2 \cdot F(m)^2 \cdot F(n)^2} \\
& \quad \times \left\{ \sin^2 \left(\frac{\pi m_1}{N_1} \right) \left\{ 1 - \cos \left(2\pi m \circ n \mp \frac{2\pi n_1}{N_1} \right) \right\} \right. \\
& \quad \quad \left. - \sin \left(\frac{\pi m_1}{N_1} \right) \sin \left(\frac{\pi n_1}{N_1} \right) \left\{ \cos \left(\frac{\pi(m_1 + n_1)}{N_1} \right) - \cos \left(2\pi m \circ n \pm \frac{\pi(m_1 - n_1)}{N_1} \right) \right\} \right\} \\
& \quad + (L_1, N_1, m_1, m_2, n_1, n_2 \leftrightarrow L_2, N_2, m_3, m_4, n_3, n_4). \tag{E.5}
\end{aligned}$$

Again by shifting m and using the approximations (E.3), we can rewrite it as

$$\frac{27g^2}{512N^2} \sum_{m,n} \frac{1 - \cos(2\pi m \circ n)}{F(m)^2 \cdot F(n)^2}. \tag{E.6}$$

(d) **Diagram with two 4-boson vertex V_{4b}**

$$- \frac{45g^2}{256N^2} \sum_{m,n} \frac{1 - \cos(2\pi m \circ n)}{F(m)^2 \cdot F(n)^2}. \tag{E.7}$$

Summing up (a)~(d), we find that the 2-loop vacuum diagrams almost cancel. Actually, if we use the approximate values (E.4) and (E.6), we have

$$(\text{E.1}) + (\text{E.4}) + (\text{E.6}) + (\text{E.7}) = \left(\frac{1}{8} - \frac{1}{512} + \frac{27}{512} - \frac{45}{256} \right) \frac{g^2}{N^2} \sum_{m,n} \frac{1 - \cos(2\pi m \circ n)}{F(m)^2 \cdot F(n)^2} = 0. \tag{E.8}$$

This cancellation is not exact, but we can see numerically that contribution of the $O(\mathcal{F}^0)$ terms is smaller than that of the $O(\mathcal{F}^2)$ terms.

E.2 $O(\mathcal{F}^2)$

The calculation of the $O(\mathcal{F}^2)$ contribution is very tedious. Here we show only the simplest case, that is, the planar part of Fig.1 (b) :

$$\begin{aligned}
& \frac{g^2 \pi^2}{256 L^4 N^3} \sum_{m,n} \left\{ \frac{1 - \cos\left(\frac{2\pi(m_1+n_1)}{N_1}\right) \cos\left(\frac{2\pi(m_2+n_2)}{N_1}\right)}{F(m)^2 \cdot F(n)^2 \cdot (F(m+n))^2} \right. \\
& \quad \times \frac{1}{r^3 \sqrt{R}} \left(\sin\left(\frac{\pi m_1}{N_1}\right) \sin\left(\frac{\pi n_1}{N_1}\right) \cos\left(\frac{\pi(m_1+n_1)}{N_1}\right) + \sin\left(\frac{\pi m_2}{N_1}\right) \sin\left(\frac{\pi n_2}{N_1}\right) \cos\left(\frac{\pi(m_2+n_2)}{N_1}\right) \right) \\
& \quad + \frac{1 - \cos\left(\frac{2\pi(m_3+n_3)}{N_2}\right) \cos\left(\frac{2\pi(m_4+n_4)}{N_2}\right)}{F(m)^2 \cdot F(n)^2 \cdot (F(m+n))^2} \\
& \quad \times r^3 \sqrt{R} \left(\sin\left(\frac{\pi m_3}{N_2}\right) \sin\left(\frac{\pi n_3}{N_2}\right) \cos\left(\frac{\pi(m_3+n_3)}{N_2}\right) + \sin\left(\frac{\pi m_4}{N_2}\right) \sin\left(\frac{\pi n_4}{N_2}\right) \cos\left(\frac{\pi(m_4+n_4)}{N_2}\right) \right) \left. \right\} \\
& \sim \frac{g^2 \pi^2 N}{256 L^4} \int d^4 k d^4 l \left\{ \frac{1 - \cos(2\pi(k_1+l_1)) \cos(2\pi(k_2+l_2))}{F(k)^2 \cdot F(l)^2 \cdot (F(k+l))^2} \right. \\
& \quad \times \frac{1}{r^3 \sqrt{R}} (\sin(\pi k_1) \sin(\pi l_1) \cos(\pi(k_1+l_1)) + \sin(\pi k_2) \sin(\pi l_2) \cos(\pi(k_2+l_2))) \\
& \quad + \frac{1 - \cos(2\pi(k_3+l_3)) \cos(2\pi(k_4+l_4))}{F(k)^2 \cdot F(l)^2 \cdot (F(k+l))^2} \\
& \quad \left. \times r^3 \sqrt{R} (\sin(\pi k_3) \sin(\pi l_3) \cos(\pi(k_3+l_3)) + \sin(\pi k_4) \sin(\pi l_4) \cos(\pi(k_4+l_4))) \right\}.
\end{aligned} \tag{E.9}$$

Here, $k_i = m_i/N_1, k_j = m_j/N_2, l_i = n_i/N_1, l_j = n_j/N_2$ ($i = 1, 2; j = 3, 4$), and k_μ and l_μ vary from 0 to 1.

References

- [1] N.Ishibashi,H.Kawai,Y.Kitazawa and A.Tsuchiya,*A Large N Reduced Model as Superstring*, hep-th/9612115.
M. Fukuma, H. Kawai, Y. Kitazawa, A. Tsuchiya, *String Field Theory from IIB Matrix Model*, hep-th/9705128;
N. Ishibashi, S. Iso, H. Kawai, Y. Kitazawa *Wilson Loops in Noncommutative Yang Mills*;hep-th/9910004
S. Iso, H. Kawai, *Spacetime and Matter in IIB Matrix Model - gauge symmetry and diffeomorphism -*, hep-th/9903217
For review, see H.Aoki,S.Iso,H.Kawai,Y.Kitazawa,A.Tsuchiya and T.Tada, *IIB Matrix Model*, hep-th/9908038.
- [2] H. Aoki, S. Iso, H. Kawai, Y. Kitazawa, T. Tada, *Space-time Structures from IIB Matrix Model*, hep-th/9802085.
- [3] J. Nishimura, G. Vernizzi, *Spontaneous Breakdown of Lorentz Invariance in IIB Matrix Model* hep-th/0003223;
K.N. Anagnostopoulos, J. Nishimura, *A new approach to the complex-action problem and its application to a nonperturbative study of superstring theory* hep-th/0108041;
J.F. Wheeler, G. Vernizzi, *Rotational Symmetry Breaking in Multi-Matrix Models*,hep-th/0206226
J. Nishimura, *Exactly Solvable Matrix Models for the Dynamical Generation of Space-Time in Superstring Theory*, hep-th/0108070
- [4] J.Nishimura and F.Sugino, *Dynamical Generation of Four-Dimensional Space-Time in the IIB Matrix Model*, hep-th/0111102 ;

- H.Kawai, S.Kawamoto, T.Kuroki, T.Matsuo and S.Shinohara, *Mean Field Approximation of IIB Matrix Model and Emergence of Four Dimensional Space-Time*, hep-th/0204240 ;
H.Kawai, S.Kawamoto, T.Kuroki and S.Shinohara, *Improved Perturbation Theory and Four-Dimensional Space-Time in IIB Matrix Model*, hep-th/0211272.
J. Nishimura, T. Okubo, F. Sugino, *Gaussian expansion analysis of a matrix model with the spontaneous breakdown of rotational symmetry*, hep-th/0412194
Similar method has also applied to matrix quantum mechanics : D.Kabat and G.Lifschytz, *Approximations for strongly-coupled supersymmetric quantum mechanics*, hep-th/9910001
- [5] A. Connes, M. R. Douglas, A. Schwarz *Noncommutative Geometry and Matrix Theory: Compactification on Tori*; hep-th/9711162;
N. Seiberg, E. Witten *String Theory and Noncommutative Geometry* hep-th/9908142;
R. C. Myers, *Dielectric-Branes*, hep-th/9910053;
A.Yu. Alekseev, A. Recknagel, V. Schomerus, *Brane Dynamics in Background Fluxes and Noncommutative Geometry*, hep-th/0003187;
R. J. Szabo, *Quantum Field Theory on Noncommutative Spaces*, hep-th/0109162
- [6] H.Aoki,N.Ishibashi,S.Iso,H.Kawai,Y.Kitazawa and T.Tada, *Noncommutative Yang-Mills in IIB Matrix Mdel*, hep-th/9908141;
M.Li, *Strings from IIB Matrices*, hep-th/9612222.
- [7] S.Iso, Y.Kimura, K.Tanaka, K. Wakatsuki, *Noncommutative Gauge Theory on Fuzzy Sphere from Matrix Model*, hep-th/0101102;
S. Bal, H. Takata, *Interaction between two Fuzzy Spheres*, hep-th/0108002;
Y. Kitazawa, *Matrix Models in Homogeneous Spaces*, hep-th/0207115;
Y. Kimura, *On Higher Dimensional Fuzzy Spherical Branes*, hep-th/0301055;
Y. Kimura, *Myers Effect and Tachyon Condensation*, hep-th/0309082;
Y. Kimura *Nonabelian gauge field and dual description of fuzzy sphere*, hep-th/0402044;
Y. Kitazawa, Y. Takayama, D. Tomino, *Correlators of Matrix Models on Homogeneous Spaces*, hep-th/0403242
- [8] U. C. Watamura, S. Watamura, *Noncommutative Geometry and Gauge Theory on Fuzzy Sphere*, hep-th/9801195;
D. P. Jatkar, G. Mandal, S. R. Wadia, K.P. Yogendran, *Matrix dynamics of fuzzy spheres*, hep-th/0110172
P. Valtancoli, *Stability of the fuzzy sphere solution from matrix model*, hep-th/0206075;
Peter Austing, John F. Wheeler, *Adding a Myers Term to the IIB Matrix Model*, hep-th/0310170;
P.Castro-Villarreal, R.Delgadillo-Blando, B Ydri, *A Gauge-Invariant UV-IR Mixing and The Corresponding Phase Transition For $U(1)$ Fields on the Fuzzy Sphere*, hep-th/0405201
- [9] T.Imai and Y.Takayama, *Stability of Fuzzy $S^2 \times S^2$ Geometry in IIB Matrix Model*, hep-th/0312241.
- [10] T.Imai,Y.Kitazawa,Y.Takayama and D.Tomino, *Quantum Corrections on Fuzzy Sphere*, hep-th/0303120 ;
Effective Actions of Matrix Models on Homogeneous Spaces, hep-th/0307007.
- [11] Y.Kimura, *Noncommutative Gauge Theories on Fuzzy Sphere and Fuzzy Torus from Matrix Model*, hep-th/0103192.
- [12] T. Azuma, S. Bal, K. Nagao and J. Nishimura, *Phase structure of the 6d Yang-Mills-Chern-Simons model — fuzzy $S^2 \times S^2$ versus fuzzy S^2 —*, in preparation
- [13] T. Azuma, S. Bal, K. Nagao and J. Nishimura, *Nonperturbative studies of fuzzy spheres in a matrix model with the Chern-Simons term*, hep-th/0401038;
Absence of a fuzzy S^4 phase in the dimensionally reduced 5d Yang-Mills-Chern-Simons model, hep-th/0405096;
Dynamical aspects of the fuzzy CP^2 in the large- N reduced model with a cubic term, hep-th/0405277.